

## Supporting Information

# Enhanced Durability of Polymer Electrolyte Membrane Fuel Cells by Functionalized 2D Boron Nitride Nanoflakes

*Keun-Hwan Oh<sup>1,+</sup>, Dongju Lee<sup>2,+</sup>, Min-Ju Choo<sup>3</sup>, Kwang Hyun Park<sup>3</sup>, Seokwoo Jeon<sup>2</sup>, Soon  
Hyung Hong<sup>2,\*</sup>, Jung-Ki Park<sup>3,\*</sup>, and Jang Wook Choi<sup>1,4,\*</sup>*

<sup>1</sup>Graduate School of EEWS (Energy, Environment, Water, and Sustainability), Korea  
Advanced Institute of Science and Technology, Daejeon, 305-701 (Korea)

<sup>2</sup>Department of Material Science and Engineering, Graphene Research Center (GRS), and  
KAIST Institute NanoCentury, Korea Advanced Institute of Science and Technology,  
Daejeon, 305-701 (Korea)

<sup>3</sup>Department of Chemical and Biomolecular Engineering, Korea Advanced Institute of  
Science and Technology, Daejeon, 305-701 (Korea)

<sup>4</sup>Center for Nature-inspired Technology (CNiT), KAIST Institute NanoCentury, Korea  
Advanced Institute of Science and Technology, Daejeon, 305-701 (Korea)

### Corresponding Author

\*Email: shhong@kaist.ac.kr, jungpark@kaist.ac.kr, jangwookchoi@kaist.ac.kr

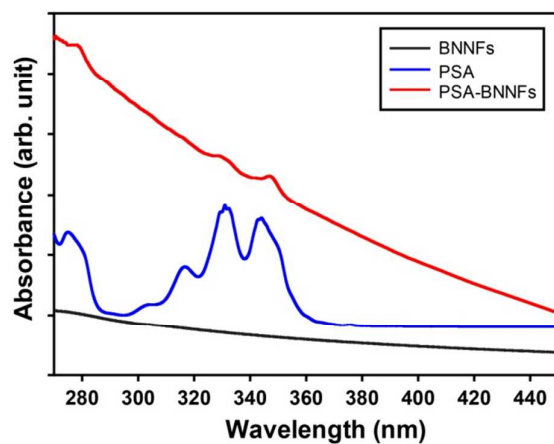


**Figure S1.** UV-Vis spectra of BNNFs, PSA, and PSA-BNNFs. The spectrum of PSA exhibited characteristic peaks at 278, 311, 327, and 339 nm, which are attributed to the electron delocalization in the pyrene rings.<sup>[S1]</sup> In the spectrum of PSA-BNNFs, most of the PSA peaks were collapsed owing to the PSA-BNNFs interaction.<sup>[S2]</sup>

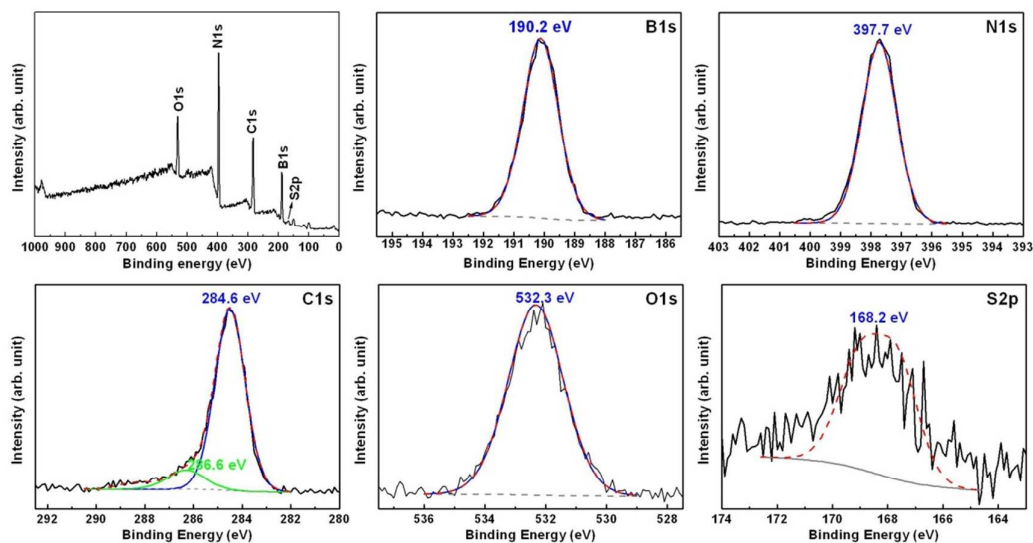


**Figure S2.** XPS survey scan and elemental spectra of PSA-BNNFs.

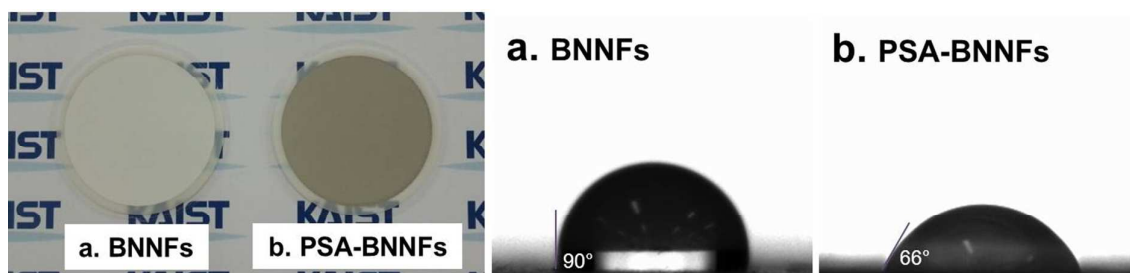


**Figure S3.** Water contact angles of (a) BNNFs and (b) PSA-BNNFs thin films.

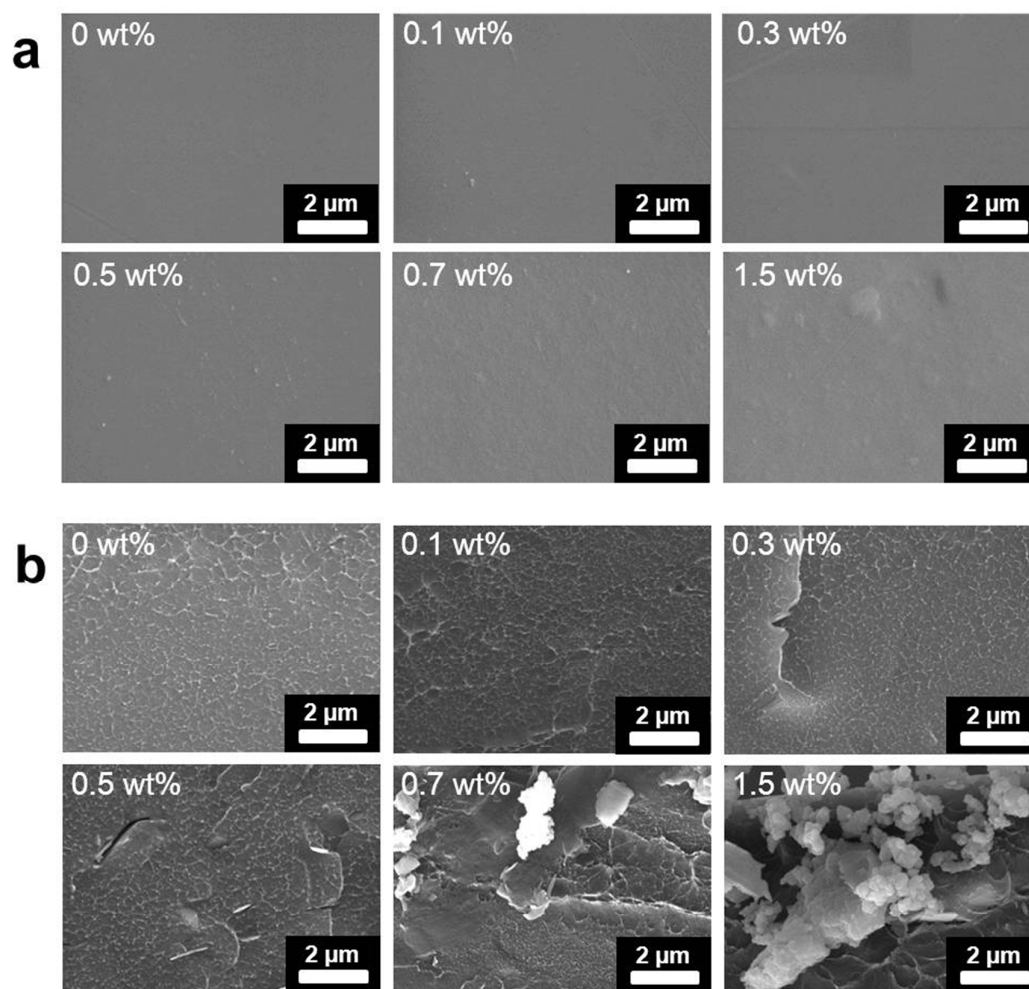


**Figure S4.** (a) Surface and (b) cross-sectional SEM images of the composite membranes with various PSA-BNNFs contents.

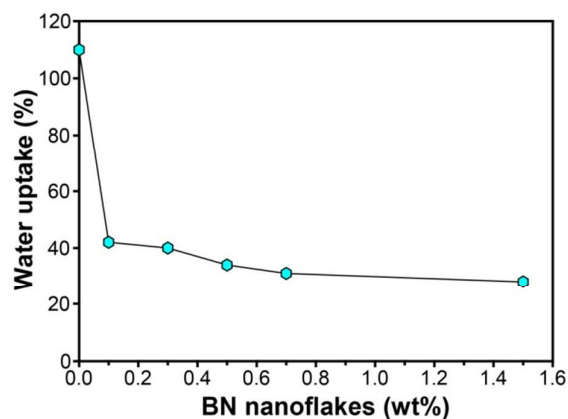


**Figure S5.** Water uptake of the composite membranes with various PSA-BNNFs contents.

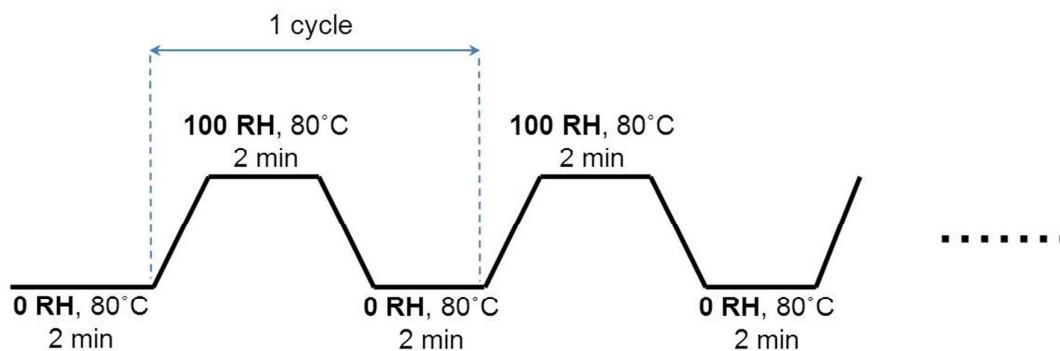


**Figure S6.** A wet/dry cycling protocol for long-term operations.

Sample	Initial dimension			Final dimension			Dimensional change (%)		
	$l(mm)$	$t(\mu m)$	$v(mm^3)$	$l(mm)$	$t(\mu m)$	$v(mm^3)$	$\Delta l$	$\Delta t$	$\Delta v$
sPEEK				$64.5 \pm 0.4$	$54.8 \pm 0.2$	$5.7 \pm 0.09$	$29 \pm 1.6$	$37 \pm 2.2$	$128 \pm 10$
0.1wt.% PSA-BNNFs/sPEEK				$57.5 \pm 0.3$	$48.0 \pm 0.2$	$4.0 \pm 0.06$	$15 \pm 1.3$	$20 \pm 2.0$	$59 \pm 8$
0.3wt.% PSA-BNNFs/sPEEK	$50.0 \pm 0.3$	$40.0 \pm 0.5$	$2.5 \pm 0.07$	$56.0 \pm 0.3$	$48.4 \pm 0.2$	$3.8 \pm 0.06$	$12 \pm 1.3$	$21 \pm 2.0$	$52 \pm 7$
0.5wt.% PSA-BNNFs/sPEEK				$55.5 \pm 0.4$	$48.4 \pm 0.2$	$3.7 \pm 0.07$	$11 \pm 1.5$	$21 \pm 2.0$	$49 \pm 6$
0.7wt.% PSA-BNNFs/sPEEK				$55.5 \pm 0.3$	$48.0 \pm 0.3$	$3.7 \pm 0.06$	$11 \pm 1.3$	$20 \pm 2.3$	$48 \pm 7$
1.5wt.% PSA-BNNFs/sPEEK				$55.5 \pm 0.3$	$48.4 \pm 0.2$	$3.7 \pm 0.06$	$11 \pm 1.3$	$21 \pm 2.0$	$49 \pm 6$

**Table S1.** Dimensional changes of the composite membranes with various PSA-BNNFs contents. The error ranges indicate the entire data ranges obtained from 10 different samples.

Sample	$R_m (\Omega \text{ cm}^2)$		$R_{cl} (\Omega \text{ cm}^2)$		$R_{ct} (\Omega \text{ cm}^2)$		$C_{ct} (\text{F cm}^{-2})$	
	Before cycling	After cycling	Before cycling	After cycling	Before cycling	After cycling	Before cycling	After cycling
Bare sPEEK	0.297	0.445	0.065	0.067	0.213	0.215	0.920	0.931
0.3wt% PSA-BNNFs/sPEEK	0.293	0.299	0.066	0.069	0.201	0.207	0.891	0.900

**Table S2.** Resistances and capacitances of the bare sPEEK and composite (0.3 wt%) membranes before and after 500 and 950 wet/dry cycles.

$R_{cl}$  was determined from the impedance at 0.6 V by analyzing the linear region starting from the greater intercept on the real axis. In this linear region, the overall impedance can be correlated with  $R_{cl}$ , the double layer capacitance ( $C_{dl}$ ) of the CL, and frequency ( $\omega$ ) based on the following relation [S3].

$$|Z| = \sqrt{\frac{R_{cl}}{C_{dl}}} \omega^{-\frac{1}{2}}$$

By fitting the curves in the linear regions to the above equation, the  $R_{cl}$  of the bare sPEEK and composite membranes was determined, and those data are summarized in Table S2. The quite persistent  $R_{cl}$  before and after cycling supports that the observed performance decay originates from the membrane degradation, not the CL degradation. The charge transfer resistance,  $R_{ct}$ , before and after cycling was also determined (Table S2) by fitting the semicircles in the Nyquist plots to an equivalent circuit (Figure 5f inset in the main text) in which oxygen-reduction reaction is described by a parallel combination of  $R_{ct}$  and constant phase element (CPE).  $R_{ct}$  turned out almost identical before and after the wet/dry cycles for both membrane cases (bare sPEEK:  $0.213 \rightarrow 0.215 \Omega \text{ cm}^2$ , 0.3 wt% composite membrane:  $0.201 \rightarrow 0.207 \Omega \text{ cm}^2$ ), indicating that CL degradation is not very prominent.

[S1] Wu, X.; Shi, G. *J. Mater. Chem.* **2005**, *15*, 1833-1837.

[S2] Pagona, G.; Tagmatarchis, N.; Fan, J.; Yudasaka, M.; Iijima, S. *Chem. Mater.* **2006**, *18*, 3918-3920.

[S3] Kim, H.-T.; Song, K.-Y.; Reshetenko, T. V.; Han, S.-I.; Kim, T.-Y.; Cho, S.-Y.; Min, M.-K.; Chai, G.-S.; Shin, S.-C. *J. Power Sources* **2009**, *193*, 515-522.